Interface structure of half-metallic Heusler alloy Co_2MnSi thin films facing an MgO tunnel barrier determined by x-ray magnetic circular dichroism

Toshiaki Saito* and Toshikazu Katayama
Department of Physics, Faculty of Science, Toho University, Funabashi 274-8510, Japan

Takayuki Ishikawa and Masafumi Yamamoto†
Division of Electronics for Informatics, Hokkaido University, Sapporo 060-0814, Japan

Daisuke Asakura and Tsuneharu Koide
Photon Factory, IMSS, High Energy Accelerator Research Organization, Tsukuba 305-0801, Japan

Yoshio Miura and Masafumi Shirai
Research Institute of Electrical Communication, Tohoku University, Sendai 980-8577, Japan
(Received 14 March 2010; published 15 April 2010)

Using x-ray absorption spectroscopy and x-ray magnetic circular dichroism, we performed an element-specific investigation of the spin magnetic moments (m_{spin}) of Mn and Co of Co_2MnSi ultrathin layers grown on an Fe underlayer to stabilize the ferromagnetism and facing an MgO barrier. The experimentally observed dependence of the m_{spin} values of Co and Mn on the Co_2MnSi layer thickness in the ultrathin region is qualitatively in good agreement with the one theoretically obtained for a MnSi-terminated interface of the Co_2MnSi layer facing an MgO barrier. This clarification would provide a strong basis for further advancement of applications of half-metallic Heusler alloy electrodes into spintronic devices.

DOI: 10.1103/PhysRevB.81.144417 PACS number(s): 75.70.−i, 68.35.Ct, 75.50.Cc, 73.20.−r

I. INTRODUCTION

Spintronic devices that manipulate the spin degree of freedom of the electron are being extensively studied,[1] which could lead to future electron devices featuring nonvolatility and reconfigurability. Half-metallic ferromagnets (HMFs) are characterized by an energy gap for one spin direction, providing complete spin polarization at the Fermi level (E_F).[2] Because of this characteristic, HMFs are one of the promising ferromagnetic electrode materials in spintronic devices. One Co-based Heusler alloy (Co_2YZ, where Y is usually a transition metal and Z is a main-group element) in particular, Co_2MnSi, has attracted much interest[3–10] because of its theoretically predicted half-metallic nature[11,12] with a large energy gap of 0.81 eV (Ref. 12) for its minority-spin band and because of its high Curie temperature of 985 K.

For magnetic tunnel junctions (MTJs) with half-metallic electrodes, Mavropoulos *et al.*[13] theoretically predicted a crucial role of the minority-spin interface states at the half-metallic electrode/oxide junction in spin-dependent tunneling characteristics for antiparallel (AP) magnetization alignment. Furthermore, Co_2YZ layers in epitaxial Co_2YZ/MgO heterostructures with the (001) basal plane have two possible terminated interfaces with an MgO barrier, i.e., the YZ- and Co-terminated interfaces. It has been predicted by first-principles calculations that the interfacial spin polarization of Co_2MnSi facing an MgO barrier strongly depends on the terminated interface structure of Co_2MnSi at Co_2MnSi/MgO junctions.[14–17] Thus, identifying the interface structure at Co_2YZ/MgO junctions with well-controlled interfaces is essential. We have recently proposed and developed fully epitaxial MTJs with Co_2YZ alloy electrodes in combination with an MgO(001) barrier[5–8] and demonstrated a high tunneling magnetoresistance (TMR) ratio of up to 1135% at 4.2 K with a substantially decreased one of 236% at room temperature (RT) for epitaxial Co_2MnSi/MgO/Co_2MnSi MTJs.[8] The strong temperature (T) dependence of the tunneling resistance for AP magnetization alignment resulted in the observed strong T dependence of the TMR ratio for epitaxial Co_2MnSi-MgO MTJs.[5,7] Similar T dependence of the TMR ratio was observed also for Co_2MnSi/AlO_x/Co_2MnSi MTJs.[4] On the basis of the dynamical mean-field theory, Chioncel *et al.*[10] attributed the strong T dependence of the TMR ratio to nonquasiparticle states, which appear in the half-metallic gap of Co_2MnSi and degrade the spin polarization remarkably with increasing T. In recent hard x-ray photoelectron spectroscopic measurements,[18] however, no distinct T dependence has been observed for the valence band of Co_2MnSi. We therefore need an alternative explanation of the T dependence of the TMR ratio observed in the MTJs with Co_2MnSi electrodes. Ishikawa *et al.* experimentally suggested the critical role played by interface states for minority spins existing around E_F of Co_2MnSi electrodes facing an MgO barrier to explain the spin-dependent dI/dV versus V characteristics.[7] On the other hand, recent high-angle annular dark-field scanning-transmission electron-microscopy measurements suggest that the terminating interface of the Co_2MnSi layer facing an MgO barrier consists of the layer next to the Co layer, including site disorder between the first two atomic layers at the junction,[19] where the MgO barrier was deposited by magnetron sputtering. Given this background, in order to further advance the applicability of half-metallic Co_2YZ into spintronic devices, it is essential to develop a means for determining nondestructively the interface structure and clarify the structural, electronic, and magnetic properties of the interfacial region between Co_2YZ electrodes and tunneling barrier.

Our objective in the present study was to elucidate the interface structure of Co_2MnSi electrodes facing an MgO barrier by experimental investigation along with a theoretical analysis. For this purpose, we performed an element-specific investigation of the spin magnetic moments (m_{spin}) of Mn and Co of Co_2MnSi in the interfacial region facing an MgO barrier by means of x-ray absorption spectroscopy (XAS) and x-ray magnetic circular dichroism (XMCD), which are very effective techniques for exploring the electronic and magnetic states of the interfacial region of ferromagnetic thin films facing an oxide or semiconductor.[20–26] To specifically measure the interfacial region by XAS and XMCD, we prepared ultrathin Co_2MnSi layers facing an MgO barrier with Co_2MnSi thicknesses (t) down to one monolayer, where one monolayer of Co_2MnSi consists of a Co plane and a MnSi plane and corresponds to half the unit cell of Co_2MnSi. To stabilize the ferromagnetic order of the ultrathin Co_2MnSi layers, the Co_2MnSi layers were grown on an Fe underlayer. The experimentally obtained dependence of m_{spin} of Mn and Co of Co_2MnSi in the Fe/CMS (t)/MgO as a function of t was analyzed theoretically, taking into consideration the influence of both interfaces with the lower Fe layer and upper MgO barrier.

II. EXPERIMENTAL

The sample layer structure was as follows: (from the substrate side) MgO buffer (10 nm)/Fe underlayer (50 nm)/Co_2MnSi (t)/MgO barrier (2 nm)/Ru cap (2 nm), grown on an MgO(001) single-crystal substrate, where t=177 ML (50 nm), 4 ML (1.13 nm), 2 ML (0.565 nm corresponding to a unit cell), and 1 ML (0.283 nm). The preparation of the samples is described in detail elsewhere.[25,26] The Co_2MnSi film was deposited at RT by magnetron sputtering and subsequently annealed *in situ* at 325 °C for 15 min. To ensure there would be no Fe diffusion into the ultrathin Co_2MnSi film, we used a relatively low annealing temperature of 325 °C.[27] The MgO barrier was deposited at RT by electron-beam (EB) evaporation. The composition of the Co_2MnSi films used in this study was determined as $Co_2Mn_{0.91}Si_{0.93}$, which was slightly Co rich against the Mn and Si compositions. From *in situ* reflection high-energy electron diffraction (RHEED) observations, we confirmed that all the layers in the Fe/Co_2MnSi/MgO with t=2 and 1 ML grew epitaxially with the (001) basal plane as in the case for t=4 ML.[25] We also observed 1/2-order superlattice reflections along the $[110]_{CMS}$ direction in the RHEED patterns for these films annealed at 325 °C, indicating that the Co_2MnSi film with t=2 and 1 ML had the $L2_1$ structure as that for t=4 ML did.[25] XAS and XMCD spectra were measured at RT with the total electron yield method by using circularly polarized synchrotron radiation at the KEK Photon Factory (BL-11A). The degree of circular polarization of incident light was set to 87% (±4%). XAS spectra for opposite magnetic-field directions were acquired consecutively with the photon helicity fixed. XMCD is defined as the difference between the two spectra with the photon helicity parallel (μ_+) and antiparallel (μ_-) to the 3d majority-spin directions.

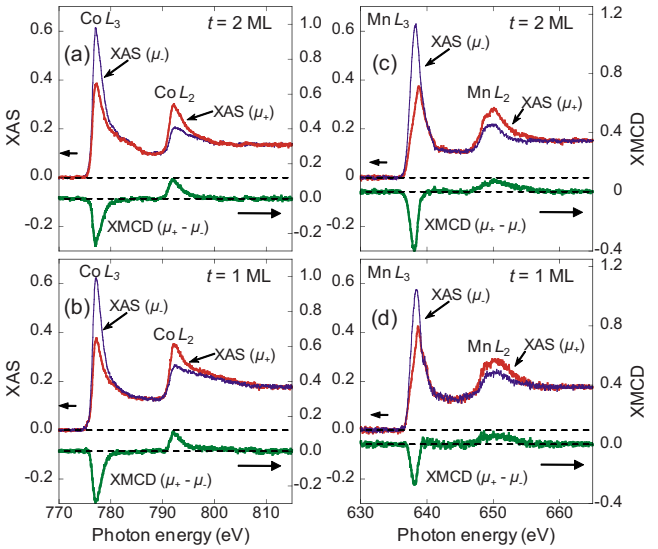

FIG. 1. (Color online) XAS and XMCD spectra for Fe/Co_2MnSi (t)/MgO layer structures with t=2 and 1 ML at RT. A magnetic field B=±3 T strong enough to saturate the sample's magnetization was applied perpendicular to the film surface of samples. [(a) and (b)] At the Co-$L_{2,3}$ edges. [(c) and (d)] At the Mn-$L_{2,3}$ edges. In each figure, the left- and right-hand side labels represent the normalized XAS and XMCD values, respectively.

III. RESULTS

A. X-ray magnetic circular dichroism spectra

Figure 1 shows XAS and XMCD spectra for Fe/Co_2MnSi (t)/MgO at the Co-$L_{2,3}$ and Mn-$L_{2,3}$ edges for t=2 and 1 ML. The XAS and XMCD intensities were normalized by the Co-L_3 (Mn-L_3) XAS total peak intensity, i.e., $\mu_+ + \mu_-$, with a linear background subtracted in the XAS. We first describe how the XAS and XMCD spectrum at the Co-$L_{2,3}$ changes with decreasing t. In the referenced XAS spectrum for t=4 ML in Ref. 25, a small distinct shoulder appeared at the higher photon energy (about 3 eV) side of the Co-L_3 peak, which is characteristic of Co_2YZ with the $L2_1$ structure.[22–24,26] The shoulder structure became weaker and the Co-L_3 peak width became smaller for t=2 ML [Fig. 1(a)] than those for t=4 ML. For t=1 ML, the shoulder structure disappeared and a much narrower Co-L_3 peak was observed [Fig. 1(b)], reflecting the significant interfacial effect and some possible structural disorder in the ultrathin 1-ML-thick Co_2MnSi film. We then describe how the XAS and XMCD spectrum at the Mn-$L_{2,3}$ changes with decreasing t. For t=4 ML in Ref. 25, a broad structure appeared in the XAS and XMCD spectra in the higher photon energy (about 2~10 eV) region of the Mn-L_3 XAS peak and a doublet structure appeared in the Mn-L_2 region in the XAS spectrum, which are characteristic of Co_2YZ with the $L2_1$ structure.[22–24,26] The broad structure in XAS spectra, however, disappeared for t=2 and 1 ML [Figs. 1(c) and 1(d)], reflecting again a considerable interfacial effect. For these Co_2MnSi films with t ranging from 4 to 1 ML, XMCD signals were noticeably observed, which implies the existence of substantial magnetic moments on Co and Mn, even for t =1 ML with an assist from the molecular field of the Fe

TABLE I. The spin (m_{spin}) and orbital (m_{orb}) magnetic moments of Co and Mn atoms deduced from the XMCD spectra observed for Fe/Co_2MnSi (t ML)/MgO layer structures with thickness t of 1, 2, 4, and 177 ML (50 nm).

	Co		Mn	
t (ML)	m_{spin} (μ_B)	m_{orb} (μ_B)	m_{spin} (μ_B)	m_{orb} (μ_B)
177[a]	1.16 ± 0.1	0.02 ± 0.1	2.95 ± 0.1	0.08 ± 0.1
4[a]	1.25	0.06	3.35	0.05
2	1.37	0.18	3.92	0.28
1	1.48	0.15	2.74	0.03

[a]References 25 and 26.

underlayer. The Mn-edge XMCD signal for $t=1$ ML [Fig. 1(d)], however, is smaller than those of the Co_2MnSi films with $t=4$ and 2 ML, which indicates a reduction in the magnetic moment of Mn for $t=1$ ML. The absence of the characteristic multiplet structures of CoO_x (Ref. 20) and MnO (Ref. 25) in the XAS spectrum and the noticeably observed XMCD signals for all Co_2MnSi films also rule out the possibility of oxidization of Co and Mn atoms.

For a more precise analysis of the XAS and XMCD spectra, we used the sum rules,[28] from which one can evaluate m_{spin} and the orbital magnetic moment (m_{orb}) of Mn and Co as

$$m_{orb} = -\frac{4}{3}\frac{q}{r} n_h \mu_B, \tag{1}$$

$$m_{spin} + 7m_T^z = -\frac{6p-4q}{r} n_h \mu_B, \tag{2}$$

where r is the XAS energy integral, $r=\int_{L_3+L_2}(\mu_+ + \mu_-)d\omega$, q is the XMCD energy integral over the $L_{2,3}$ edges, and $q=\int_{L_3+L_2}(\mu_+ - \mu_-)d\omega$. The p is the XMCD energy integral over the L_3 edge, expressed as $p=\int_{L_3}(\mu_+ - \mu_-)d\omega$, and $m_T^z = \langle T_z \rangle \mu_B/\hbar$ with $\langle T_z \rangle$ being the expectation value of the intra-atomic magnetic dipole operator.[28] For the evaluation of m_{spin} and m_{orb} of Co and Mn in Co_2MnSi films facing an MgO barrier, we assumed, on the basis of a band-structure calculation,[29] a $3d$ hole number (n_h) of 4.52 for Mn and 2.24 for Co and ignored the term $\langle T_z \rangle$, assuming this value to be very small. For Mn, the m_{spin} obtained should be corrected for the effect of jj mixing arising from $2p$-$3d$ electrostatic interaction.[22,30] However, we estimated m_{spin} of Mn in Co_2MnSi films using the bare spin sum rules because a correction factor of Mn in Co_2MnSi with the $L2_1$ structure is not accurately known.

The obtained experimental m_{spin} and m_{orb} values of Co and Mn for Co_2MnSi films with $t=2$ and 1 ML and with $t=4$ ML and $t=177$ ML (50 nm) (Refs. 25 and 26) as references are listed in Table I, and the experimental m_{spin} values are plotted in Fig. 2. Most importantly, the experimental m_{spin} values of both Co and Mn considerably increased with decreasing t from 4 to 1 ML with the exception of the decreased m_{spin} value of Mn for $t=1$ ML. Although slight increases in these values for $t=4$ ML compared with those for $t=177$ ML have been observed (8% and 14% increases for Co and Mn, respectively),[26] we found that the m_{spin} values definitely increase with decreasing t for samples with $t=2$ and 1 ML except for the m_{spin} value of Mn for $t=1$ ML. These behaviors clearly demonstrate interfacial effects in these heterostructures. The m_{spin} value of Co increased with decreasing t from $1.16\mu_B$ for $t=177$ ML to $1.48\mu_B$ for $t=1$ ML (a 28% increase). In addition, the m_{spin} value of Mn increased with decreasing t from $2.95\mu_B$ for $t=177$ ML to $3.92\mu_B$ for $t=2$ ML (a 33% increase) while it dropped to $2.74\mu_B$ for $t=1$ ML.

On the other hand, the m_{orb} values for Co and Mn were very small for $t=4$ and 177 ML [$0.02-0.06\mu_B$ and $0.05-0.08\mu_B$, respectively]. This indicates that the orbital

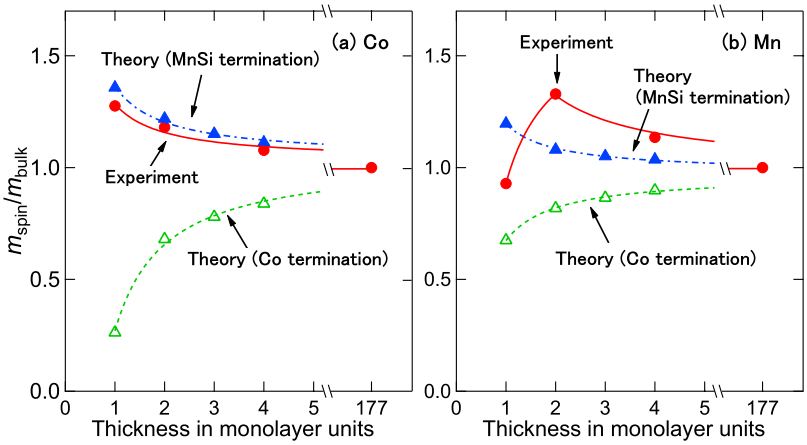

FIG. 2. (Color online) Experimental m_{spin} for (a) Co and (b) Mn of Co_2MnSi films in Fe/Co_2MnSi (t)/MgO layer structures as a function of t for $B=3$ T at RT (solid circles), where the experimental m_{spin} values are normalized by their respective experimental values for the Co_2MnSi film with $t=177$ ML (50 nm) [m_{bulk}(experiment for $t=177$ ML)$=1.16\mu_B$ for Co and $2.95\mu_B$ for Mn]. Theoretically calculated values of the averaged m_{spin} (m_{ave}) of Co and Mn in the Fe(001)/Co_2MnSi (t)/MgO layer structures with the MnSi/MgO interface (solid triangles) and Co/MgO interface (open triangles) are also shown as a function of t, where the theoretical m_{spin} values are normalized by their respective theoretical m_{spin} values for bulk Co_2MnSi [m_{bulk}(theory)$=0.935\mu_B$ for Co and $3.310\mu_B$ for Mn].

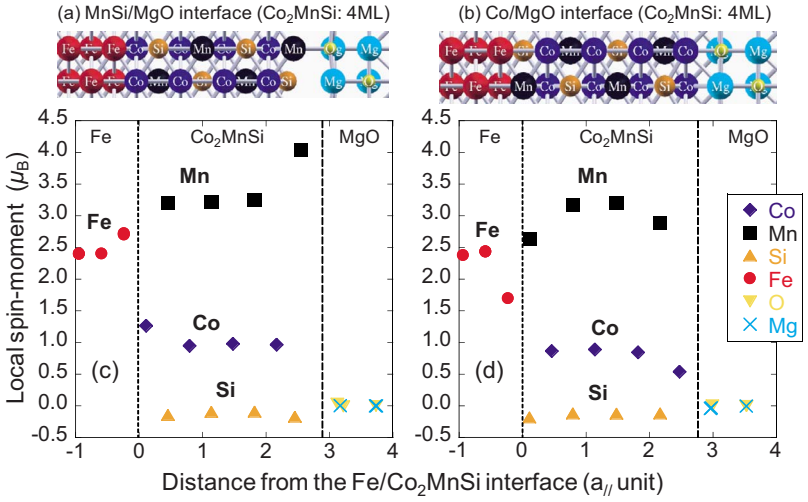

FIG. 3. (Color online) Schematic representations of Fe(001)/Co_2MnSi (4 ML)/MgO layer structures with (a) the MnSi/MgO interface and (b) the Co/MgO interface, respectively. The local spin moments (m_{spin}) projected on to each atomic sphere in the layer structures with (c) the MnSi/MgO interface and (d) the Co/MgO interface, respectively, as a function of distance from the Co_2MnSi/MgO junction.

magnetic moments are quenched due to the cubic symmetry in Co_2MnSi with the $L2_1$ structure, though these values are larger than the theoretically predicted ones of about $0.02\mu_B$ for Co and about $0.008\mu_B$ for Mn in bulk Co_2MnSi with the $L2_1$ structure.[12] However, except for the m_{orb} value of Mn for $t=1$ ML, some increases in the m_{orb} values of Co and Mn were observed when t was further decreased to 2 and 1 ML, as shown in Table I. The increased m_{orb} values have also been observed for Co_2MnSi thin films grown on GaAs(001) substrates.[23] Comparing the t dependence of m_{spin} and that of m_{orb}, the former is more distinct. Furthermore, the accuracy of the m_{spin} values is higher that of the m_{orb} values because of their one-order higher values. Thus, the t dependence of m_{spin} is more suitable than that of m_{orb} for comparisons with theoretical analyses that take interfacial effects at both sides into account.

B. First-principles calculation

To reveal the terminated interface structure of Co_2MnSi layers facing an MgO barrier through comparison with the experimental results, we performed first-principles calculations for supercells consisting of Fe, Co_2MnSi, and MgO, using the density-functional theory within the generalized-gradient approximation for the exchange-correlation energy.[31] We adopted plane-wave-basis sets along with the ultrasoft pseudopotential method using the quantum code ESPRESSO.[32] The spin-orbit interaction and the noncollinear spin structures were neglected in our calculations. The number of k points was taken to be $10\times10\times1$ for all cases, and Methfessel-Paxton smearing with a broadening parameter of 0.01 Ryd was used. The cut-off energy for the wave function and charge density was set to 30 and 300 Ryd, respectively. The Fe(001)/Co_2MnSi (t)/MgO ($t=1-4$ ML) layer structure was constructed in a tetragonal supercell. We prepared the supercell containing eight atomic layers of bcc-Fe, 1–4 ML of Co_2MnSi and eight atomic layers of MgO. The in-plane lattice parameter of the supercell was fixed at 0.399 nm, which corresponds to $a_0/\sqrt{2}$, where $a_0=0.565$ nm is the lattice constant of the bulk Co_2MnSi.

Figures 3(a) and 3(b) show schematic representations of Fe(001)/Co_2MnSi (4 ML)/MgO layer structures with the MnSi/MgO interface and the Co/MgO interface, respectively. Figures 3(c) and 3(d) show the local m_{spin} projected on to each atomic sphere in the structures as a function of distance from the Co_2MnSi/MgO junction. As can be seen in Figs. 3(c) and 3(d), the local m_{spin} of Mn at the MnSi/MgO interface increases compared with that in the interior region of the Co_2MnSi layer, while the local m_{spin} of Co at the Co/MgO interface decreases compared with that in the interior region of the Co_2MnSi layer, as reported in a previous theoretical work.[17]

At the MnSi/MgO interface, as shown schematically in Fig. 3(a), the difference in the covalent bond radius between Si (0.111 nm) and Mn (0.139 nm) causes relaxation of the interfacial structure. The Si atom moves away from the MgO side and only the Mn atom makes a bond with the O atom. In our previous study,[15] we showed that this relaxation thermodynamically stabilizes the MnSi/MgO interface rather than the Co/MgO interface. However, the relaxation weakens the local bonding between the Co_2MnSi layer and the MgO layer, causing dangling bonds for the interfacial atoms. Since electrons in the dangling bond states are energetically unstable, they tend to localize in order to reduce the exchange-correlation energy, which is associated with the increase in the local m_{spin} of the interfacial Mn atom. This increase is achieved by a charge transfer from the minority-spin to the majority-spin states. On the other hand, at the Co/MgO interface, the interfacial Co atom makes a strong bond with the O atom. The strong bonding causes charge transfer from the Co layer to the MgO layer owing to the large electron affinity of O atoms. We confirmed that E_F of the local density of states (LDOS) of Co at the Co/MgO interface shifts toward the lower energy side compared to that in bulk Co_2MnSi (see Fig. 2 of Ref. 14). Since bulk Co_2MnSi has no minority-spin state at E_F, reduction in the occupied states in the interfacial LDOS is significant for the majority-spin states, resulting in the decrease in the local m_{spin} of Co at the Co/MgO interface.

Next, we discuss the magnetic properties of the Fe(001)/Co_2MnSi interface. The local m_{spin} of Co at the Fe/Co interface ($1.27\mu_B$) is larger than that of Co in bulk Co_2MnSi ($0.935\mu_B$), as shown in Fig. 3(c), because the m_{spin} of Co in bulk Co_2MnSi is smaller than that in B2-type CoFe ($1.72\mu_B$). Furthermore, the local m_{spin} of Mn at the Fe/MnSi

interface ($2.63\mu_B$) is smaller than that of Mn in bulk Co_2MnSi ($3.31\mu_B$), as shown in Fig. 3(d). Since the Fe/MnSi interface can be seen locally as Fe_2MnSi, the local m_{spin} of Mn at the Fe/MnSi is close to the m_{spin} of Mn in bulk Fe_2MnSi ($2.83\mu_B$) rather than to that of Mn in bulk CMS.

The theoretically calculated values of the averaged m_{spin} (m_{ave}) of (a) Co and (b) Mn in the Fe(001)/Co_2MnSi (t)/MgO as a function of t are also plotted in Fig. 2 in comparison with the experimental m_{spin}, where the solid and open triangles show data for Co_2MnSi/MgO junctions with the MnSi/MgO and Co/MgO interfaces, respectively. Importantly, the theoretically obtained t dependence of m_{ave} of Co and Mn in the Fe(001)/Co_2MnSi (t)/MgO is qualitatively different between the MnSi/MgO and Co/MgO interface models. The theoretical m_{ave} values for both Co and Mn for the layer structure with the MnSi/MgO and Co/Fe interfaces (Co/MgO and MnSi/Fe interfaces) increases (decreases) with decreasing t. This dependence originates from the increased (decreased) local m_{spin} of Mn and Co at the MnSi/MgO and Co/Fe interfaces (the Co/MgO and MnSi/Fe interfaces), respectively, as described above.

IV. DISCUSSION

The experimentally observed dependence of the m_{spin} values of Co and Mn on t is qualitatively in good agreement with the one theoretically obtained with a MnSi-terminated interface of the Co_2MnSi layer facing an MgO barrier, indicating that the interface structure at the Co_2MnSi/MgO junction is a MnSi-terminated one. This finding is consistent with the theoretical prediction that a MnSi-terminated interface with MgO is thermodynamically stable compared with a Co-terminated interface.[15] The good agreement also indicates that the epitaxial Co_2MnSi/MgO heterostructures prepared using a combination of magnetron sputtering for Co_2MnSi and EB evaporation for MgO, except the 1-ML Co_2MnSi one, have well-controlled structures in the interfacial region.

We now discuss a possible origin of the decrease in m_{spin} of Mn for $t=1$ ML. Taking into account that (i) Co_2MnSi films deposited at RT and successively annealed *in situ* even at 550–600 °C do not reach a thermal equilibrium state,[8] (ii) the Mn_{Co} antisite, where a Co site is replaced by a Mn atom, has the lower formation energy among the several kinds of defects,[33,34] and (iii) the degree of structural order should be lower for an extremely thin Co_2MnSi film with $t=1$ ML, Mn_{Co} antisites may exist with a certain probability for the prepared Co_2MnSi films annealed at 325 °C, in particular, for the Co_2MnSi film with $t=1$ ML. The possible Mn_{Co} antisite in the 1-ML-thick Co_2MnSi grown on an Fe layer may couple antiferromagnetically with the surrounding Fe and Co atoms as the Mn_{Co} antisite in bulk Co_2MnSi couple antiferromagnetically with the surrounding Mn atoms in the neighboring MnSi layer,[33] resulting in the decreased m_{ave} of Mn for $t=1$ ML. However, the good qualitative agreement between the experimental dependence of the m_{spin} of Co and Mn down to $t=2$ ML and the theoretically obtained one indicates that the first two layers facing an MgO barrier in the 2-ML and 4-ML Co_2MnSi retained a higher degree of structural order compared with that of the 1-ML Co_2MnSi facing an MgO barrier.

We next discuss possible origins of the observed enhancement of m_{orb} of Co for $t=2$ and 1 ML and that of Mn for $t=2$ ML. One possible reason is the lower cubic symmetry at the interfaces, which results in reduced quenching of m_{orb}. Another is the increased m_{spin} for these ultrathin films that were caused by the interfacial effect, which induces the enhanced orbital moments through the spin-orbit interaction.[35] Given this consideration, the significantly reduced orbital moment of Mn for $t=1$ ML is consistent with the decreased m_{spin} of Mn for $t=1$ ML. A full understanding of the t dependence of m_{orb} is, however, beyond the scope of this study.

Recently, it has been proposed that the insertion of an ultrathin Co_2CrAl layer between a Co_2MnSi electrode and an MgO barrier can derive the half-metallic character at the interface.[15] The transfer of Cr $3d$ electrons from the minority- to the majority-spin states acts to reconstruct the half-metallic gap in the interfacial region. As a result, the local m_{spin} of the interfacial Cr atom is increased significantly from the bulk value. The results of the present study suggest that element-specific investigations of m_{spin} at the Cr-$L_{2,3}$ edges by means of XMCD would be useful for examining the theoretical prediction regarding the effect of the inserted Co_2CrAl layer.

V. SUMMARY

In summary, the comparison of the experimental results, in particular, the increase in the spin magnetic moments of Co and Mn in the Fe/Co_2MnSi/MgO epitaxial layer structure with decreasing Co_2MnSi thickness, with the theoretical analysis clearly revealed that the terminated interface of the Co_2MnSi layer at the Co_2MnSi/MgO junction was a MnSi-terminated interface. This result indicates that element-specific evaluations of spin magnetic moments in the interfacial region along with a theoretical analysis are highly useful for determining nondestructively the interfacial termination layer of Heusler alloy thin films facing an MgO barrier.

ACKNOWLEDGMENTS

This work was partly supported by Grants-in-Aid for Scientific Research on Priority Area "Creation and Control of Spin Current" (Grant Nos. 19048001 and 19048002) and by a Grant-in Aid for Scientific Research (A) (Grant No. 20246054) from MEXT, Japan.

*saito@ph.sci.toho-u.ac.jp
†yamamoto@nano.ist.hokudai.ac.jp

[1] I. Žutić, J. Fabian, and S. Das Sarma, Rev. Mod. Phys. **76**, 323 (2004).
[2] R. A. de Groot, F. M. Mueller, P. G. van Engen, and K. H. J. Buschow, Phys. Rev. Lett. **50**, 2024 (1983).
[3] S. Kämmerer, A. Thomas, A. Hütten, and G. Reiss, Appl. Phys. Lett. **85**, 79 (2004).
[4] Y. Sakuraba, M. Hattori, M. Oogane, Y. Ando, H. Kato, A. Sakuma, T. Miyazaki, and H. Kubota, Appl. Phys. Lett. **88**, 192508 (2006).
[5] T. Ishikawa, T. Marukame, H. Kijima, K.-i. Matsuda, T. Uemura, M. Arita, and M. Yamamoto, Appl. Phys. Lett. **89**, 192505 (2006).
[6] T. Ishikawa, S. Hakamata, K.-i. Matsuda, T. Uemura, and M. Yamamoto, J. Appl. Phys. **103**, 07A919 (2008).
[7] T. Ishikawa, N. Itabashi, T. Taira, K.-i. Matsuda, T. Uemura, and M. Yamamoto, Appl. Phys. Lett. **94**, 092503 (2009).
[8] T. Ishikawa, H.-x. Liu, T. Taira, K.-i. Matsuda, T. Uemura, and M. Yamamoto, Appl. Phys. Lett. **95**, 232512 (2009).
[9] S. J. Hashemifar, P. Kratzer, and M. Scheffler, Phys. Rev. Lett. **94**, 096402 (2005).
[10] L. Chioncel, Y. Sakuraba, E. Arrigoni, M. I. Katsnelson, M. Oogane, Y. Ando, T. Miyazaki, E. Burzo, and A. I. Lichtenstein, Phys. Rev. Lett. **100**, 086402 (2008).
[11] S. Ishida, S. Fujii, S. Kashiwagi, and S. Asano, J. Phys. Soc. Jpn. **64**, 2152 (1995).
[12] S. Picozzi, A. Continenza, and A. J. Freeman, Phys. Rev. B **66**, 094421 (2002).
[13] Ph. Mavropoulos, M. Ležaić, and S. Blügel, Phys. Rev. B **72**, 174428 (2005).
[14] Y. Miura, H. Uchida, Y. Oba, K. Nagao, and M. Shirai, J. Phys.: Condens. Matter **19**, 365228 (2007).
[15] Y. Miura, H. Uchida, Y. Oba, K. Abe, and M. Shirai, Phys. Rev. B **78**, 064416 (2008).
[16] B. Hülsen, M. Scheffler, and P. Kratzer, Phys. Rev. Lett. **103**, 046802 (2009).
[17] A. Sakuma, Y. Toga, and H. Tsuchiura, J. Appl. Phys. **105**, 07C910 (2009).
[18] K. Miyamoto, A. Kimura, Y. Miura, M. Shirai, M. Ye, Y. Cui, K. Shimada, H. Namatame, M. Taniguchi, Y. Takeda, Y. Saitoh, E. Ikenaga, S. Ueda, K. Kobayashi, and T. Kanomata, Phys. Rev. B **79**, 100405(R) (2009).
[19] T. Miyajima, M. Oogane, Y. Kotaka, T. Yamazaki, M. Tsukada, Y. Kataoka, H. Naganuma, and Y. Ando, Appl. Phys. Express **2**, 093001 (2009).
[20] T. Saito, T. Katayama, Y. Kurosaki, M. Endo, S. Saito, T. Kamino, K. Kobayashi, Y. Suzuki, T. Nagahama, S. Yuasa, T. Koide, T. Shidara, H. Manaka, and H. Tokano, J. Magn. Magn. Mater. **272-276**, E1489 (2004).
[21] K. Miyokawa, S. Saito, T. Katayama, T. Saito, T. Kamino, K. Hanashima, Y. Suzuki, K. Mamiya, T. Koide, and S. Yuasa, Jpn. J. Appl. Phys., Part 2 **44**, L9 (2005).
[22] J. Schmalhorst, S. Kämmerer, M. Sacher, G. Reiss, A. Hütten, and A. Scholl, Phys. Rev. B **70**, 024426 (2004).
[23] W. H. Wang, M. Przybylski, W. Kuch, L. I. Chelaru, J. Wang, Y. F. Lu, J. Barthel, H. L. Meyerheim, and J. Kirschner, Phys. Rev. B **71**, 144416 (2005).
[24] N. D. Telling, P. S. Keatley, G. van der Laan, R. J. Hicken, E. Arenholz, Y. Sakuraba, M. Oogane, Y. Ando, and T. Miyazaki, Phys. Rev. B **74**, 224439 (2006).
[25] T. Saito, T. Katayama, T. Ishikawa, M. Yamamoto, D. Asakura, and T. Koide, Appl. Phys. Lett. **91**, 262502 (2007).
[26] T. Saito, T. Katayama, A. Emura, N. Sumida, N. Matsuoka, T. Ishikawa, T. Uemura, M. Yamamoto, D. Asakura, and T. Koide, J. Appl. Phys. **103**, 07D712 (2008).
[27] S. Yuasa, T. Katayama, T. Nagahama, A. Fukushima, H. Kubota, Y. Suzuki, and K. Ando, Appl. Phys. Lett. **87**, 222508 (2005).
[28] C. T. Chen, Y. U. Idzerda, H.-J. Lin, N. V. Smith, G. Meigs, E. Chaban, G. H. Ho, E. Pellegrin, and F. Sette, Phys. Rev. Lett. **75**, 152 (1995).
[29] I. Galanakis, see Ref. 29 in Ref. 22.
[30] Y. Teramura, A. Tanaka, and T. Jo, J. Phys. Soc. Jpn. **65**, 1053 (1996).
[31] J. P. Perdew, K. Burke, and M. Ernzerhof, Phys. Rev. Lett. **77**, 3865 (1996).
[32] S. Baroni, A. Dal Corso, S. de Gironcoli, and P. Giannozzi, http://www.pwscf.org
[33] S. Picozzi, A. Continenza, and A. J. Freeman, Phys. Rev. B **69**, 094423 (2004).
[34] B. Hülsen, M. Scheffler, and P. Kratzer, Phys. Rev. B **79**, 094407 (2009).
[35] M. Tischer, O. Hjortstam, D. Arvanitis, J. Hunter Dunn, F. May, K. Baberschke, J. Trygg, J. M. Wills, B. Johansson, and O. Eriksson, Phys. Rev. Lett. **75**, 1602 (1995).